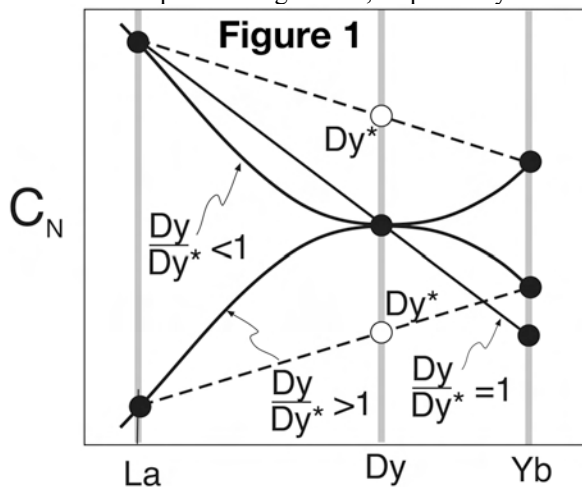


**A New Look at the Origin and Evolution of Mare Basalts using REE Profiles.** C. R. Neal<sup>1</sup> and J. P. Davidson<sup>2</sup>,  
<sup>1</sup>Dept. of Civil Eng. & Geological Sciences, University of Notre Dame, Notre Dame, IN 46556, USA ([neal.1@nd.edu](mailto:neal.1@nd.edu)). <sup>2</sup>Dept. of Earth Sciences, Durham University, Durham, DH1 3LE, United Kingdom ([j.p.davidson@durham.ac.uk](mailto:j.p.davidson@durham.ac.uk)).

**Introduction:** The rare earth elements (REEs) are a useful suite of elements for investigating magma petrogenesis. They are usually presented as chondrite- or primitive mantle normalized plots to remove the Oddo-Harkins effect. The nature of the REE profile can yield information on magma generation and/or magma evolution processes. However, comparison of large quantities of REE data through comparison of profiles is difficult; it is normally done by using La/Yb or La/Sm to examine the overall slope of the REE pattern and the slope of the light REE, respectively.

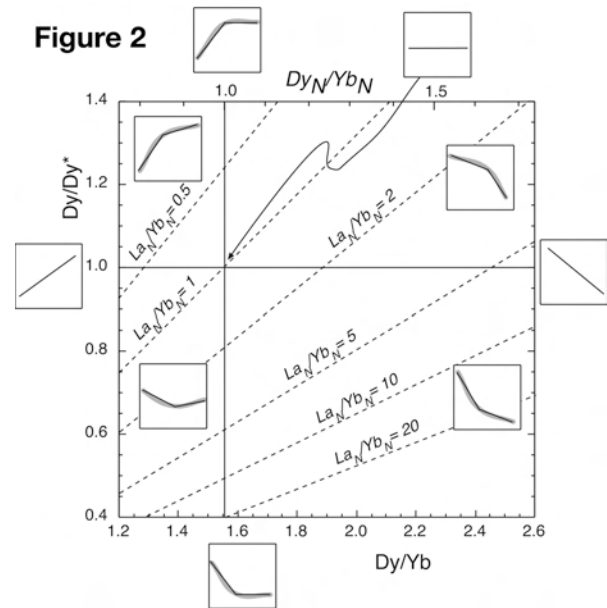


The parameter  $Dy/Dy^*$  is the measured value of Dy, a representative middle REE, compared with the value interpolated between La and Yb on a REE plot (Fig. 1) [1]. It is essentially a measure of the "concavity" of a REE pattern. The use of  $Dy/Dy^*$  as a proxy for shape, allows us to compare large amounts of REE data, which can be difficult using standard REE patterns.  $Dy/Dy^*$  is calculated in the following way:

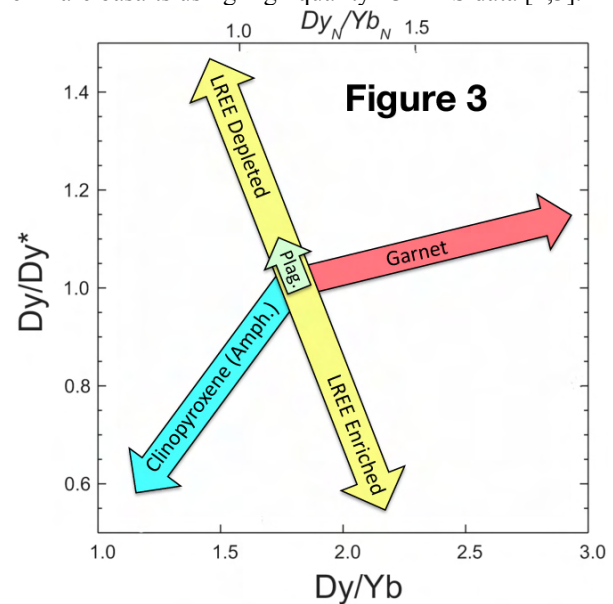
$$\frac{Dy}{Dy^*} = \frac{Dy_N}{La_N^{4/13} * Yb_N^{9/13}}$$

where "N" represents the normalized value.

If  $Dy/Dy^*$  is combined with  $Dy/Yb$  (representing the slope of the middle-to-heavy REE pattern), REE patterns can effectively be classified by shape (Fig. 2). The shape of the REE pattern is controlled by the mineralogy of the source, the partial melting process, and post-magma generation processes. In essence the REE profile represents an imprint of the processes/minerals that have affected an igneous rock from source to solidification. Such controls are shown in Figure 3 and the applicability of this approach has been used by [1] to examine the petrogenesis of volcanic suites from

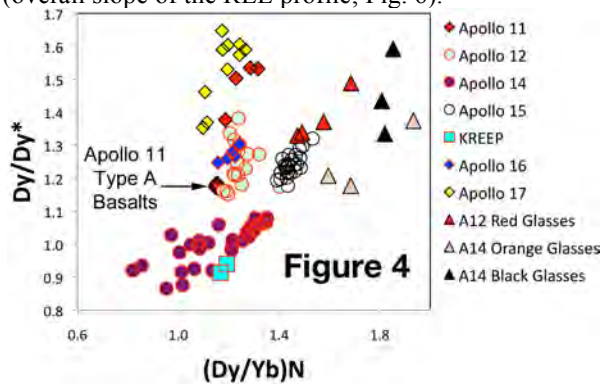


different arc systems. We present here the first effort in using this new approach to understand the petrogenesis of mare basalts using high quality ICP-MS data [2,3].



**Results & Discussion:** In this study we focus on the REE profiles of mare basalts from every type returned from the Moon, including "new" basalts from Apollo 16 reported by [3] and volcanic glasses that were suspected of originating within the garnet stability field [2]. We examine the basalt suite not only using  $Dy/Dy^*$  and  $(Dy/Yb)_N$  (Fig. 4) but also  $(Sm/Eu)_N$

(measure of any Eu anomaly; Fig. 5) and  $(La/Yb)_N$  (overall slope of the REE profile; Fig. 6).



The mare basalts form a general trend in Figure 4 that is distinct from the general negative correlation shown by MORBs and OIBs. The low-Ti basalts from Apollo 12, 14, and 15 suggest a strong clinopyroxene control. Predictably, Apollo 14 “high-Al” basalts plot close to KREEP and form 3 general groups (e.g., [4]). This plot also shows similarities and differences of source regions between the different basalts. Apollo 14 and 15 basalts plot on their own, suggesting derivation from distinct sources. Although the A-14 basalts plot close to KREEP, this is generally controlled by assimilation (e.g., [4,8,9]), although KREEP does affect the source regions of these basalts [10]. This plot also displays a distinction between the A-11 Type A (high-K) basalts and A-11 Type B1 basalts having the highest  $Dy/Dy^*$  ratio; Type B3 is intermediate. The only A-12 feldspathic basalt 12038 [5] does not plot with the other A-12 basalts – it falls within the A-15 olivine normative basalt field (white circles).

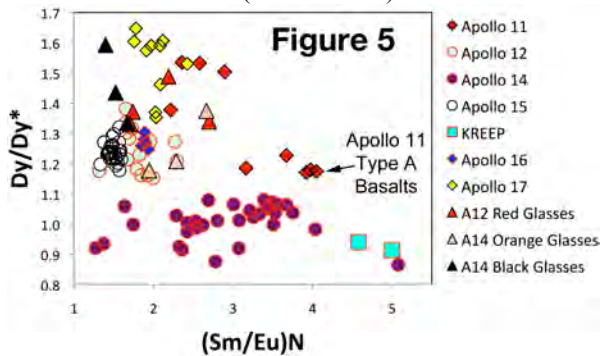


Figure 5 shows relationships between the shape of the REE pattern and the magnitude of the negative Eu anomaly in mare basalts. The influence of KREEP on A-14 and A-11 Type A basalts is again shown, but this influence is not as marked as expected in the A-14 basalts from previous work using whole-rock data [6-9]. What is shown here is the influence of plagioclase fractionation, which forms a slight positive trend in Fig. 5, on the evolution of the A-14 high-Al basalts in addition to KREEP assimilation. What is also evident

is the lack of plagioclase influence on the evolution of other mare suites.

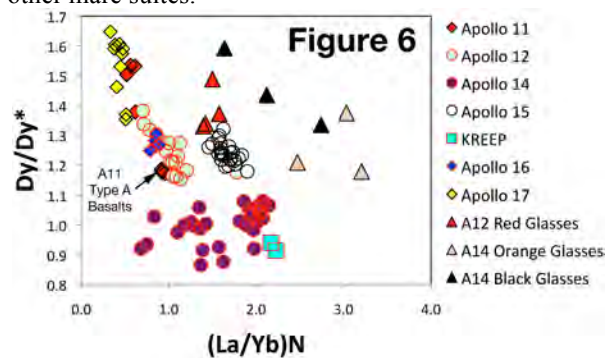


Fig. 6 shows correlations between REE profile shape and slope. KREEP influence on the A-14 high-Al basalts is evident, and the 3 compositional groups (see [4]) are seen. A-12 feldspathic basalt 12038 plots with the A-15 olivine-normative basalts. Apollo 11, 12, 16 & 17 basalts form a general negative trend.

The plots demonstrate that the high-Ti basalts are generally derived from LREE-depleted sources, whereas the low-Ti basalts generally originated from LREE-enriched sources. Influence of KREEP on different suites can be seen in Figs. 4-6 and the influence of Cpx is seen in Fig. 4 (positive trends) especially in the low-Ti basalts. The glasses appear to be unaffected by the KREEP influence. Influence of garnet in magma petrogenesis results in shifts to higher  $(Dy/Yb)_N$  and  $(La/Yb)_N$  in Figs. 4 & 6 [1]. It is evident that garnet was not involved in the petrogenesis of the mare basalts suites used in this study. However, the glasses reported by [2] to be derived from a garnet-bearing source (A-14 black & orange; A-12 red) plot to the right of the mare basalts (Fig. 4), consistent with garnet involvement in their petrogenesis.

**Conclusions.** Using the REE profiles of mare basalts as shown above is extremely useful in examining petrogenetic models. High quality data are critical in this endeavor. The relationships here show the importance of plagioclase, Cpx, and KREEP in the evolution of some of the mare basalt suites, and the influence of garnet (and not KREEP) in some volcanic glasses. Further work is underway to substantiate these preliminary conclusions.

**References:** [1] Davidson J.P. et al. (2012) *EPSL* (under review). [2] Neal C.R. (2001) *JGR* **106**, 27865-27885. [3] Fagan A.L. & Neal C.R. (2012) *LPSC* **43**. [4] Neal C.R. & Kramer G.Y. (2006) *Am. Mineral.* **91**, 1521-1535. [5] Neal C.R. et al. (1994) *Meteoritics* **29**, 334-348. [6] Dickinson T. et al. (1985) *Proc. LPSC* **15**, C365-C374. [7] Shervais J. et al. (1985) *Proc. LPSC* **15**, C375-C395. [8] Neal C.R. et al. (1988) *Proc LPSC* **18**, 139-153. [9] Neal C.R. et al. (1989) *Proc. LPSC* **19**, 147-161. [10] Hui H. & Neal C.R. (2012) *LPS* **43**.